RF and IF mixer optimum matching impedances extracted by large-signal vectorial measurements

A. Cidronali[1], G. Loglio[1], J. Jargon[3], K.A. Remley[3], I. Magrini[1], D.DeGroot[3], D. Schreurs[4], K.C. Gupta[2], G. Manes[1]

[1]Dept. Electronics and Telecommunications University of Florence, Florence 50139 Italy;
acidronali@ing.unifi.it; fax: +39.055.494569 ; tel: +39.055.494569
[2]University of Colorado at Boulder, Dept. of Electrical and Computer Engineering, USA
[3]National Institute of Standards and Technology, Boulder, CO 80305 USA
[4]K.U.Leuven; Div. ESAT-TELEMIC, Kasteelpark Arenberg 10 , B-3001 Leuven, Belgium

***Abstract* — This paper introduces a new technique that allows us to measure the admittance conversion matrix of a two-port device, using a Nonlinear Vector Network Analyzer. This method is applied to extract the conversion matrix of a 0.2 µm pHEMT, driven by a 4.8 GHz pump signal, at different power levels, using an intermediate frequency of 600 MHz. The issue on data inconsistency due to phase randomization among different measurements is discussed and a proper pre-processing algorithm is proposed to fix the problem. The output of this work consists of a comprehensive experimental evaluation of up- and down-conversion maximum gain, stability, and optimal RF and IF impedances.**

I. Introduction

Nonlinear vector network analyzers (NVNAs) were recently introduced. They have been used to characterize and model nonlinear microwave devices and circuits [1-4]. The purpose of this paper is to apply large-signal vectorial measurements to the optimum design of frequency converters. Our approach will allow us to skip the use of nonlinear device models and large-signal analysis by means of the experimental determination of the conversion matrix [5-7]. The results of [6] effectively describe how to apply such a matrix to mixer design. In the present paper is introduced a detailed conditioning process in order to avoid phase ambiguity that may arise in the approach described in [7]. The paper is organized as follows. The characterization method is described and applied to a pHEMT under large signal pumping, with a number of experimental results describing the potential of this approach for mixer design.

II. Measurement Setup

The NVNA consists of a 4-channel data acquisition system and provides magnitude and phase values of the incident and scattered complex wave variables at both ports of the device on a user-defined frequency grid. In particular, our set-up consists of two RF sources, a DC power supply, four directional couplers, an RF to IF down converter and a data acquisition system [8]. The two RF sources can be combined to supply the desired excitations at port 1 or port 2. An appropriate amplitude and phase calibration procedure allows the correction of the "raw" quantities. The set-up is shown in Fig. 1, where a large signal is applied to the DUT's port 1 while a second signal, namely a small level signal is switched to port 1 and port 2 by an external switch. The NVNA is able to measure both the harmonics of the large signal and the mixing products, if the calibration grid contains the frequencies of interest.

Although the user can define any frequency (fundamental, 2nd harmonic, ...) and variable (a1, a2, v1, v2, ...) to be the phase reference, phase-locking to a signal at a frequency different from the lowest one would bring an ambiguity in the phase values of signals at lower frequencies. This results in the need for a proper processing of the measured data that will be dealt in the next session.

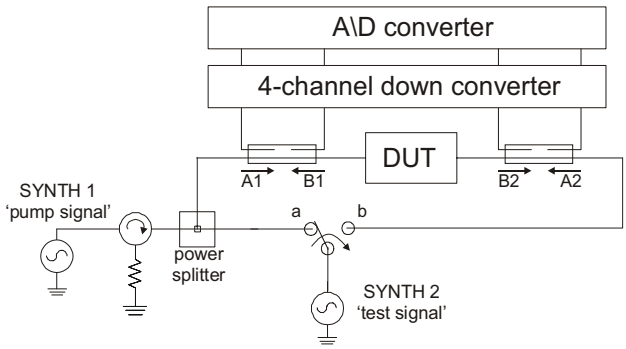

Fig. 1. Set-up adopted for the conversion matrix extraction based on NVNA (the bias part of the set is not shown).

III. Extraction of the Conversion Matrix

Let us consider the DUT pumped at port 1 by a large signal voltage V_P, whose fundamental frequency is ω_P. If small-signal voltage excitations are added at both ports, with frequencies ω_0 near any harmonic of the pump, then current responses will arise. The relationships relating the current and voltage phasors at these frequencies are linear, and they are ruled by the conversion matrix:

$$\mathbf{I} = [\mathbf{Y}] \cdot \mathbf{V}$$

Work partially supported by an agency of the U.S. Government. Not subject to U.S. Copyright.

The symbol [**Y**] represents the conversion matrix, which is, in fact, a linearization of the DUT, under the large-signal state, with respect to the small signals. The current and voltage column vectors are defined so that they contain the intermodulation components at the frequencies $\omega_k = k\omega_P + \omega_0$, with $k = -N, \ldots, 0, \ldots, N$ and at both ports:

$$\mathbf{I} = (I^*_{1,-N}, \ldots, I_{1,0}, \ldots, I_{1,N}, I^*_{2,-N}, \ldots, I_{2,0}, \ldots, I_{2,N})^{\mathrm{T}};$$

$$\mathbf{V} = (V^*_{1,-N}, \ldots, V_{1,0}, \ldots, V_{1,N}, V^*_{2,-N}, \ldots, V_{2,0}, \ldots, V_{2,N})^{\mathrm{T}}.$$

This implies that the local oscillator pump takes part of the linearized system. Let us remark for now that, as a straightforward consequence of it, the matrix [**Y**] will depend on the parameter of the pump voltage excitation. If a number of current-and-voltage vector pairs are collected, resulting from a proper number of '*M*' different experiments, provided that the conversion matrix is the same, this allows us to find the matrix [**Y**]. Tiling the current and voltage columns matrices we get

$$[\mathbf{I}^{(1)}, \ldots, \mathbf{I}^{(M)}] = [\mathbf{Y}] \cdot [\mathbf{V}^{(1)}, \ldots, \mathbf{V}^{(M)}]$$

and finally

$$[\mathbf{Y}] = [\mathbf{I}^{(1)}, \ldots, \mathbf{I}^{(M)}] \cdot [\mathbf{V}^{(1)}, \ldots, \mathbf{V}^{(M)}]^{-1},$$

where the vector superscript indicates one of the $M = 2 \cdot (2N+1)$ experiments.

Two important things are worth remarking: firstly, in order to assure that the voltage matrix to be inverted is non-singular, measurements are performed by applying the small signal at a different frequency, or to a different port of the network, in each different experiment. Secondly, in order to assure that the matrix [**Y**] is the same all over the experiments, the local oscillator pump voltage excitation must be the same for each measurement, according to the above discussion. That is to say, all the pump voltage harmonics at the two ports must be represented by identical voltage phasors, with identical amplitudes and phases. An uncertainty of the latter may be due to the NVNA set-up as recalled above.

The identity of amplitudes is easily obtained by applying a constant pump power level all over the experiments, as the small signal is assumed not to influence the large-signal behaviour. The identity of phases, however, requires a little more attention. In fact, in a set of experiments, the phases of pump voltage phasors are randomly distributed. A data pre-processing is required in order to realign phases. As the steady-state condition is assumed, no additional information is required, but just a change in the time reference system. In a given experiment '*m*', once the pump voltage fundamental frequency phasor is read, its time-domain representation can be written:

$$v_P^{(m)}(t) = |V_P| \exp(j\omega_P t + j\phi_P^{(m)}).$$

Then, a new time reference system is chosen so that

$$v_P^{(m)}(t') = |V_P| \exp(j\omega_P t' + j\phi_0),$$

the arbitrary angle ϕ_0 being constant over the experiments. In order to make it true, a relationship will exist to determine the time reference shift:

$$t' = t + (\phi_P^{(m)} - \phi_0)/\omega_P = t + \Delta t^{(m)}.$$

This shift must be applied to each current and voltage phasor of the experiment *m*; then, the generic phasor $X_{l,k}^{(m)}$ at the port *l* and at the radial frequency ω_k will have the following time domain representation in the new reference:

$$x_{l,k}^{(m)}(t') = \left|X_{l,k}^{(m)}\right| \exp(j\omega_k (t' - \Delta t^{(m)}) + j\angle X_{l,k}^{(m)}),$$

where *X* can be replaced with either *V* or *I*. It can be easily shown that it is equivalent to using the following frequency domain formula:

$$X'^{(m)}_{l,k} = X_{l,k}^{(m)} \exp(-j(\phi_P^{(m)} - \phi_0) \cdot \omega_k / \omega_P),$$

the prime indicating that the phasor is relative to the new time-reference-system. Fig. 2 offers a qualitative insight in the application of this method, by means of an example with arbitrary sine waves at two different frequencies and with unrelated phases. In particular, the lower frequency signal represents the reference used by the NVNA and the higher frequency signal represent the pump signal. The amplitude differences between sinewaves have been artificially introduced for the sake of the clarity; this is obviously absent in the experiments under discussion.

Once the phasors have been pre-processed in this way, we can correctly extract the conversion matrix in the way previously discussed.

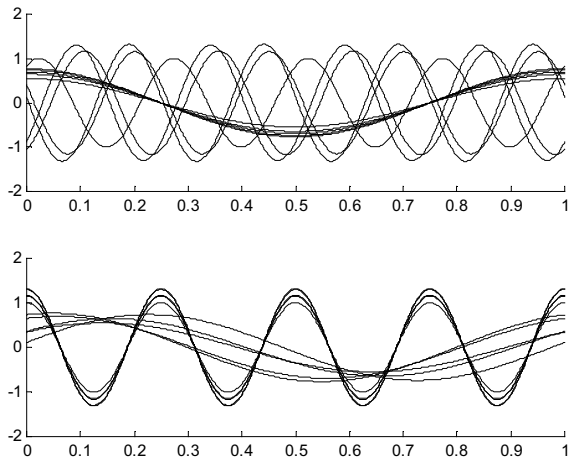

Fig. 2. Example of phase realignment method: time-domain signals aligned to the lowest frequency (top) and aligned to the pump signal (bottom) pre-processing data

IV. Experimental Results

The technique depicted above has been applied to extract the conversion matrix of a 0.2 µm pHEMT, for a pump signal at 4.8 GHz. The experiments have

been carried out for power levels ranging from –10 dBm to +10 dBm and for the bias points: V_D = 3 V, V_G = –0.45 V, –0.825 V, –1.2 V. The NVNA was calibrated with a 600MHz grid up to 19.8 GHz, considering 32 harmonics. In order to collect an adequate set of small signal components, a test signal of –30 dBm was repetitively applied to port 1 and then port 2 at 600 MHz, 4.2 GHz, 5.4 GHz, 9 GHz, 10.2 GHz, 13.8 GHz, 15 GHz, 18.6 GHz, and 19.8 GHz, (i.e., f_P = 4.8 GHz and f_0 = 600 MHz and N = 4). The power levels were selected by trading off between the constraints due to the linearity of the DUT and the dynamic range of the NVNA. Measurements of the currents and voltages at those frequencies were collected, obtaining the required set of data. Figs. 3-5 show some representative elements from matrices extracted with the above method, as a function of power levels.

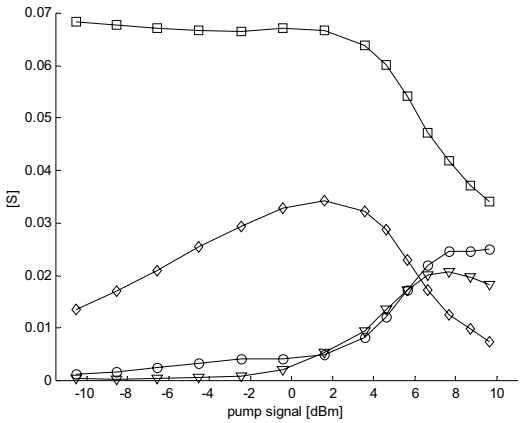

Fig. 3. Magnitude of the coefficients: y_{2111} (squares), y_{2121} (diamonds), y_{2131} (circles) and y_{2141} (triangles).

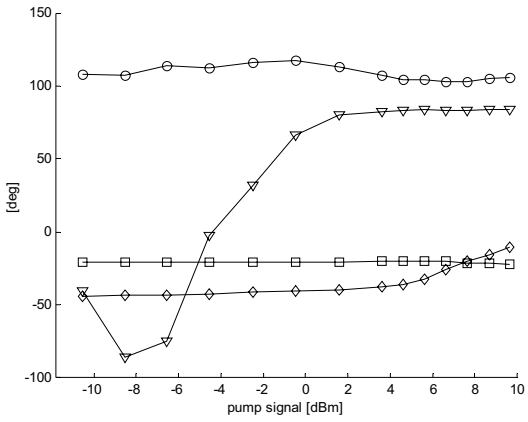

Fig. 4. Phase of the coefficients: y_{2111} (squares), y_{2121} (diamonds), y_{2131} (circles) and y_{2141} (triangles).

Figs. 3-4 report magnitude and phase values of $y_{21,11}$, $y_{21,21}$, $y_{21,31}$ and $y_{21,41}$, which represent the ratio between the current at port two at 5.4 GHz, 10.2 GHz, 15 GHz, 19.8 GHz, and the voltage at port one at 5.4 GHz.

Fig. 5 reports the up- and down-conversion related parameters from which is easy to see the optimum LO pump level required for the frequency conversion, located around +2 dBm. A two-port admittance matrix is quickly derived, after the conversion matrix has been found. In fact, if one forces the small signal to be a single tone at the input and output ports, the new matrix is found by simply retaining the corresponding rows and columns only. In practice, it is equivalent to short all the intermodulation products but the two selected frequencies, done in frequency converters. Subsequently, the analysis can proceed by using traditional small-signal amplifier theory, even though input and output frequencies are different.

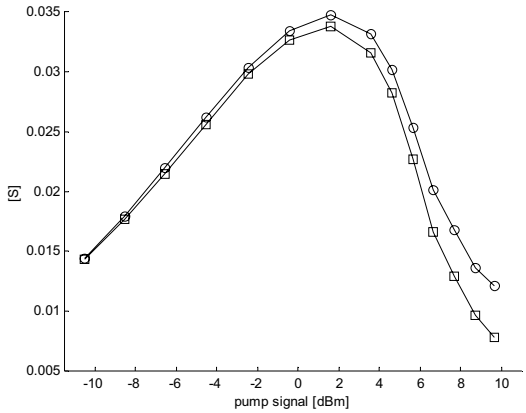

Fig. 5. Magnitude of the coefficients: y_{2110} (squares), y_{2101} (circles).

A frequency up-converter (600 MHz to 5.4 GHz) and a down-converter (5.4 GHz to 600 MHz) are considered. Maximum conversion gain (MCG) has been calculated for each pump power level, by means of well-known formulas [6], and it is shown in Fig. 6. A stability analysis was also carried out for each point, and so it was possible to distinguish whether the network was unconditionally stable, or not. If not, a maximum stable conversion gain was evaluated instead of MCG; conditionally stable points are represented as isolated stars in the graph.

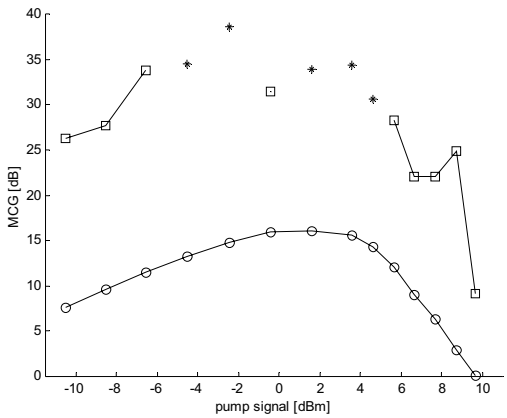

Fig. 6. Magnitude of the maximum conversion gain at 5.4 GHz ↔ 600 MHz in down-conversion (circles) and up-conversion (squares), and of maximum stable gain if not unconditionally stable (stars).

Where stability is unconditional, optimal RF-IF impedances have been calculated by imposing simultaneous conjugate match and considering them as if they were source and load impedances of a

linear two-port network. The corresponding Smith charts are reported in Figs. 7-8.

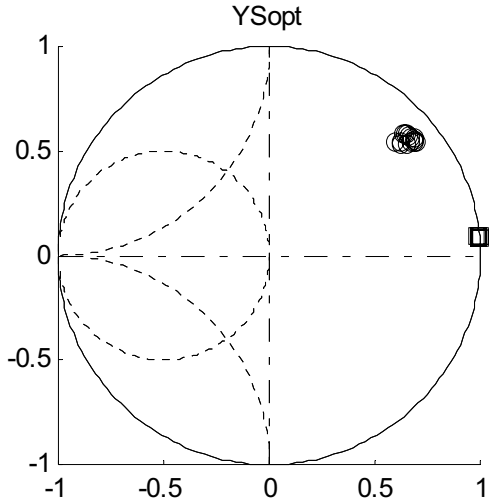

Fig. 7. Smith chart of optimal RF-IF impedances at the input port in down-conversion (circles) and up-conversion (squares).

The optimum input impedance, YSopt, shows a highly resistive behavior, slightly inductive, as expected by the physics of the input pHEMT port at 600 MHz (up-conversion), because it is mainly an open circuit with a capacitive reactive contribution. The same port shows a more meaningful capacitive behavior in the down-conversion mode and as a result the YSopt is more inductive.

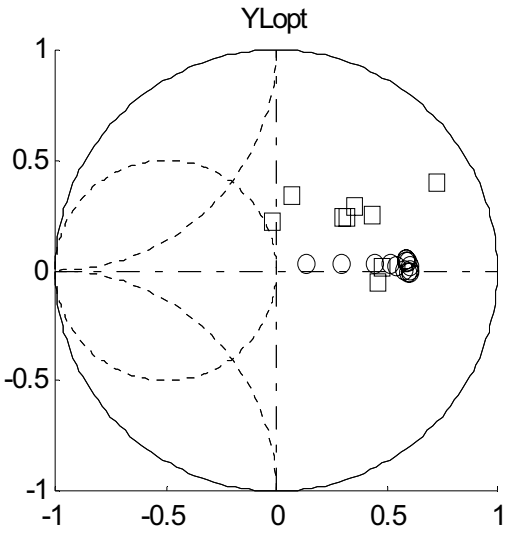

Fig. 8. Smith chart of optimal RF-IF impedances at the output port in down-conversion (circles) and up-conversion (squares) as a function of the pump level.

Similar considerations hold for the output port. The mixer design can be completed simply by the synthesis of linear networks without the requirement of nonlinear CAD tools and accurate nonlinear device model.

IV. Conclusion

We have introduced a technique to experimentally extract the conversion matrix from vectorial large-signal measurements. The method considers a pre-processing on the measured data able to avoid any phase ambiguity that may arise in multisine absolute phase measurement. It has been applied to investigate the conversion properties of a gate pumped 0.2 μm pHEMT in frequency conversion mode, as functions of the pump signal. The experimental results allow us to determine the pump level, the bias voltage and the IN/OUT terminations to optimize the design. It is believed that the method constitutes an effective improvement in the behavioral description of active devices for the mixer design.

References

[1] D. Barataud et al., "Measurement and Control of Current/Voltage Waveforms of Microwave Transistors Using a Harmonic Load-Pull System for the Optimum Design of High Efficiency Power Amplifiers," IEEE Trans. on Instrumentation and Measurement, Vol. 48, No. 4, pp. 835-842, August 1999.

[2] J. Verspecht and P. Van Esch, "Accurately characterizating of hard nonlinear behaviour of microwave components by the Nonlinear Network Measurement System: introducing the nonlinear scattering function", Proc. International Workshop on *Integrated Nonlinear Microwave and Millimiterwave Circuits*, (Duisburg, Germany), 10-11 October,1996 , pp. 17-26, Duisburg, October 1998.

[3] J. A. Jargon, K. C. Gupta, D. Schreurs, and D. C. DeGroot, "Developing Frequency-Domain Models for Nonlinear Circuits Based on Large-Signal Measurements," Proc.of the 27th General Assembly of the Intern. Union of Radio Science, CD-ROM A1.O.6, Maastricht, the Netherlands, Aug. 2002.

[4] D. Schreurs et al, "Direct extraction of the non-linear model for two-port devices from vectorial non-linear network analyzer measurements," European Microwave Conf., pp. 921-926, 1997.

[5] H.C. Torrey and C.A. Whitmer, "Crystal Rectifiers," New York: McGraw-Hill, 1948.

[6] S.A. Maas, "Nonlinear Microwave Circuits," Piscataway, N.J.: IEEE Press, 1997.

[7] A. Cidronali, K.C. Gupta, J. Jargon, K.A. Remley, D. DeGroot, G. Manes, " Extraction of Conversion Matrices for P-HEMTs based on Vectorial Large Signal Measurements", International Microwave Symposium Digest, Philadelphia, USA, June 2003.

[8] T. Van den Broeck and J. Verspecht, "Calibrated Vectorial Nonlinear Network Analyser", IEEE Microwave Theory and Techniques Symposium (MTT-S), pp. 1069-1072, 1994.